References and Notes

1. A. O. Nier, M. B. McElroy, *J. Geophys. Res.* **82**, 4341 (1977).
2. T. C. Owen *et al.*, *J. Geophys. Res.* **82**, 4635 (1977).
3. H. Nair, M. Allen, A. D. Anbar, Y. L. Yung, R. T. Clancy, *Icarus* **111**, 124 (1994).
4. V. A. Krasnopolsky, *J. Geophys. Res.* **100**, 3263 (1995).
5. The basic data on the chemical composition of Mars' atmosphere were obtained from the mass spectrometers on the Viking 1 and 2 landing probes that were used to study the upper (*1*) and lower (*2*) atmospheres. However, those mass spectrometers had been designed for masses exceeding 10 and could not detect H_2.
6. An attempt to detect H_2 on Mars by summing the Mariner 9 ultraviolet spectra resulted in an upper limit of 1.5 R to the line at 1607.5 Å that corresponded to the H_2 density of 1.1×10^5 cm^{-3} at 560 km (*53*). One R (Rayleigh) corresponds to a column production of 10^6 photons cm^{-2} s^{-1} $(4\pi$ ster$)^{-1}$.
7. Spectroscopic detection of H_2 presents some difficulties. Despite the low H_2 dissociation energy of 4.48 eV, dissociation to the ground-state H atoms is parity-forbidden, and H_2 absorbs photons only below 1108 Å in the lines of the Lyman and other band systems. The Lyman system converges to the dissociative continuum at 845 Å, which corresponds to the formation of one of the H atoms in the excited state $n = 2$. The solar radiation is weak below 1108 Å, and the fluorescence of H_2 is weak as well. Fortunately, three absorption lines of the H_2 Lyman band system are exceptionally close to the strong solar Lyman β 1025.72 Å, Lyman γ 972.54 Å, and C II 1037.02 Å lines. The differences in the wavelengths are smaller than the widths of the solar lines, and the H_2 emission lines from these three levels are much stronger than other H_2 emission lines. This effect was first observed and explained using the Apollo 17 ultraviolet spectrometer (*54*).
8. B. Blair, B. G. Anderson, Eds., *The FUSE Observer's Guide* (version 3.0, January 2001; http://fuse.pha.jhu.edu/support/guide/guide.html).
9. 1 AU (astronomical unit) is the distance between Earth and the Sun (1.5×10^8 km).
10. S. W. Bougher, S. Engel, R. G. Roble, B. Foster, *J. Geophys. Res.* **105**, 17669 (2000).
11. Eight spectra of Mars and eight foreground spectra were observed at each of six orbits. Wavelengths in each spectrum were adjusted using strong unblended lines of H, O, N, and Ar. Only one of the four telescopes was exactly pointed to Mars, and pointing of the other telescopes was less accurate because of thermal flexture. Exposures, intensities of strong lines, and the known instrument effective areas were used to determine statistical weights for averaging.
12. W. Liu, A. Dalgarno, *Astrophys. J.* **462**, 502 (1996).
13. Some other lines were considered in (*12*) for Jupiter but should be very weak on Mars.
14. The population α was calculated as

$$\alpha(J) = \frac{(2J+1)\,g_s \exp\left[-\dfrac{hcBJ(J+1)}{kT}\right]}{\Sigma\,(2J+1)\,g_s \exp\left[-\dfrac{hcBJ(J+1)}{kT}\right]}$$

where g_s is the nuclear spin statistical weight, $B = 60.853$ cm^{-1} is the H_2 ground-state rotational constant, h and k are the Planck and Boltzmann constants, respectively, and c is the speed of light.

15. The absorption cross sections σ were calculated as

$$\sigma\ (\mathrm{cm}^2\ \text{Å}) = \frac{10^8 A\lambda^4\,(2J'+1)}{8\pi c(2J''+1)}$$

Nuclear spins are the same for upper and lower states and cancel out, A is the transition probability, and λ is the wavelength in cm.

16. H. Abgrall, E. Roueff, F. Launay, J.-Y. Roncin, J.-L. Subtil, *Astron. Astrophys. Suppl. Ser.* **101**, 273 (1993).
17. H. P. Warren, J. T. Mariska, K. Wilheim, *Astrophys. J. Suppl. Ser.* **119**, 105 (1998).
18. The H_2 line at 1037.15 Å is near the solar lines at 1036.34, 1037.02, and 1037.61 Å. We fitted the observed maxima and minima of this structure in (*55*) with Gaussians and took into account the instrument resolution of 84 mÅ in (*55*) to obtain the solar intensity at 1037.15 Å.
19. P. G. Richards, J. A. Fennelly, D. G. Torr, *J. Geophys. Res.* **99**, 8981 (1994).
20. D. E. Anderson, C. W. Hord, *J. Geophys. Res.* **76**, 6666 (1971).
21. R. S. Nakata, K. Watanabe, F. M. Matsunaga, *Sci. Light* **14**, 54 (1965).
22. J. W. Chamberlain, D. M. Hunten, *Theory of Planetary Atmospheres* (Academic Press, Orlando, FL, 1987).
23. This term was calculated as

$$0.93\,\frac{(R + 160\ \mathrm{km})(2\pi RH)^{1/2}\,(1 + 9/8\lambda)}{R^2(1 + 2/\lambda)}$$

where $H = R/\lambda = 331$ km is the H_2 scale height at 160 km for 270 K, $\lambda = \gamma Mm/(RkT) = 10.73$ is the structure parameter, γ is the gravitational constant, M and m are the masses of Mars and H_2, respectively, and 0.93 is a ratio of H_2 column abundances at 160 and 140 km.

24. We deduced the following relation between τ and τ_0:

$$\tau = \frac{2}{\sqrt{\pi}}\int_0^{\infty}\left\{1 - \exp[-\tau_0 \exp(-x^2)]\right\}dx$$

which is applicable for $\tau_0 < 1$.

25. V. A. Krasnopolsky, in preparation.
26. ———, M. J. Mumma, G. R. Gladstone, *Science* **280**, 1576 (1998).
27. The heliocentric distance of Mars was 1.67 AU, $F_{10.7\ \mathrm{cm}} = 70$, and $T_\infty = 200$ K during the observation (*26*). These values are similar to those from Viking 1 and Viking 2 (*1*, *2*).
28. V. A. Krasnopolsky, *Icarus* **148**, 597 (2000).
29. $HDO/H_2O = 2\ D/H$.
30. T. Owen, J. P. Maillard, C. de Bergh, B. L. Lutz, *Science* **240**, 1767 (1988).
31. V. A. Krasnopolsky, G. L. Bjoraker, M. J. Mumma, D. E. Jennings, *J. Geophys. Res.* **102**, 6525 (1997).
32. R. Hagemann, G. Nief, E. Roth, *Tellus* **22**, 712 (1970).
33. B. M. Cheng *et al.*, *Geophys. Res. Lett.* **26**, 3657 (1999).
34. T. Fouchet, E. Lellouch, *Icarus* **144**, 114 (2000).
35. Y. L. Yung, D. M. Kass, *Science* **280**, 1545 (1998).
36. B. M. Jakosky, *J. Geophys. Res.* **95**, 1475 (1990).
37. D. E. Smith *et al.*, *Science* **284**, 1495 (1999).
38. J. W. Head, *J. Geophys. Res.* **106**, 10075 (2001).
39. J. Touma, J. Wisdom, *Science* **259**, 1294 (1993).
40. B. M. Jakosky, B. G. Henderson, M. T. Mellon, *J. Geophys. Res.* **100**, 1579 (1995).
41. L. L. Watson, I. D. Hutcheon, S. Epstein, E. M. Stolper, *Science* **265**, 86 (1994).
42. L. A. Leshin, S. Epstein, E. M. Stolper, *Geochim. Cosmochim. Acta* **60**, 2635 (1996).
43. L. A. Leshin, *Geophys. Res. Lett.* **27**, 2017 (2000).
44. H. Nair, Y. L. Yung, *Bull. Am. Astron. Soc.* **27**, (1995).
45. We obtained 10 m by integrating the data from table 1 in (*56*) and adding the data for nonthermal escape from (*57*).
46. D. M. Kass, thesis, California Institute of Technology (1999).
47. R. E. Johnson, D. Schnellenberger, M. C. Wong, *J. Geophys. Res.* **105**, 1659 (2000).
48. H. J. Melosh, A. M. Vickery, *Nature* **338**, 487 (1989).
49. J. F. Kasting, J. B. Pollack, *Icarus* **53**, 479 (1983).
50. K. Zahnle, J. F. Kasting, J. B. Pollack, *Icarus* **84**, 502 (1990).
51. This is a standard assumption for calculations of deuterium enrichment in the inner solar system.
52. G. Dreibus, H. Wänke, *Icarus* **71**, 225 (1987).
53. H. W. Moos, *J. Geophys. Res.* **79**, 2887 (1974).
54. P. D. Feldman, W. G. Fastie, *Astrophys. J.* **185**, L101 (1973).
55. W. Curdt *et al.*, *Astron. Astrophys. Suppl. Ser.* **126**, 281 (1997).
56. B. M. Jakosky, R. O. Pepin, R. E. Johnson, J. L. Fox, *Icarus* **111**, 271 (1994).
57. J. G. Luhmann, *J. Geophys. Res.* **102**, 1637 (1997).
58. Supported by the NASA FUSE Guest Investigator Program. V.A.K. thanks A. Dalgarno for consultation.

21 August 2001; accepted 16 October 2001

Mediterranean Sea Surface Radiocarbon Reservoir Age Changes Since the Last Glacial Maximum

Giuseppe Siani,[1]* Martine Paterne,[1]† Elisabeth Michel,[1]
Roberto Sulpizio,[3] Alessandro Sbrana,[4]
Maurice Arnold,[1,2] Geoffrey Haddad[5]

Sea surface reservoir ages must be known to establish a common chronological framework for marine, continental, and cryospheric paleoproxies, and are crucial for understanding ocean-continent climatic relationships and the paleoventilation of the ocean. Radiocarbon dates of planktonic foraminifera and tephra contemporaneously deposited over Mediterranean marine and terrestrial regions reveal that the reservoir ages were similar to the modern one (~400 years) during most of the past 18,000 carbon-14 years. However, reservoir ages increased by a factor of 2 at the beginning of the last deglaciation. This is attributed to changes of the North Atlantic thermohaline circulation during the massive ice discharge event Heinrich 1.

The reservoir age R_{surf} of surface ocean water (the difference between the ^{14}C age of the sea surface and that of the atmosphere) reflects the balance among ^{14}C production, CO_2 exchange between the atmosphere and ocean, and mixing with ^{14}C-depleted intermediate waters (*1*). The distribution of modern (before 1950) marine reservoir ages correlates closely with the main features of global thermohaline circulation. Surface ages vary from ~400 years in the well-ventilated gyres of the central North and South Pacific and Atlantic Ocean up to ~1200 years in the higher southern latitudes of these oceans (2). During the last deglaciation, oceanic circulation varied greatly, as did CO_2 fluxes and air-sea exchange; consequently, so did reservoir ages (1). Past reservoir ages are sparsely documented (3–5) but may vary by a factor of 2 in the North Atlantic Ocean (3) and by a factor of 5 in the deep Southwest Pacific Ocean (5). These changes are not taken into account when evaluating the oceanic paleoventilation by using ^{14}C age differences between paired benthic-planktonic foraminifera in deep-sea cores (6) or ^{14}C "projection" ages (7). Better reservoir age estimates would allow more precise constraints to be placed on the radiocarbon age calibration record below 12,000 calendar years before the present (cal yr B.P.) (8).

We have determined past R_{surf} values for the Mediterranean Sea by comparing the accelerator mass spectrometry (AMS) ^{14}C ages of monospecific planktonic foraminifera and the tephra within which they were found, in a high–sedimentation rate deep-sea core (MD 90-917) collected in the south Adriatic Sea downwind from the South Italian volcanoes (Fig. 1). Identification of the terrestrial volcanic source of the marine tephra is described in (9). ^{14}C ages of charcoals beneath volcanic deposits constrain the "atmospheric" ages of the tephra (10). Additional dates were measured on the peaks of abundance of planktonic foraminifera (9, 11). Aging of marine tephra by bioturbation (3) is not taken into account because of the high sedimentation rate in the core (~35 cm per 1000 years, except at ~8500 years B.P.) (12). To relate R_{surf} changes to climatic conditions, we used oxygen isotope ($\delta^{18}O$) values of planktonic foraminifera, together with sea surface temperatures (SSTs) determined with the modern analog technique (13) (Fig. 2).

In the Mediterranean Sea, the modern R_{surf} is 390 ± 80 years (14), similar to that of the North Atlantic Ocean (2). This similarity is due to modern oceanic circulation patterns: Atlantic surface waters from the western middle latitudes enter through the Gibraltar strait into the Mediterranean Sea, from where the surface waters rapidly overturn to the North Atlantic intermediate waters with a residence time of ~100 years (15). In the open Adriatic Sea, the present site of Mediterranean deep water formation, modern values of R_{surf} are similar to those of the Mediterranean (14). The anti-estuarine circulation pattern of the Mediterranean Sea did not change in the past 18,000 years, except during the Mediterranean sapropel event at ~8500 years B.P. (9, 13, 16, 17). This is demonstrated by unchanged surface salinity gradients between the Atlantic and the Mediterranean Sea during that time (9, 13) and by the continued presence of Mediterranean outflow water (MOW) far into the North Atlantic (16, 17). Consequently, Mediterranean Sea surface waters have recorded North Atlantic oceanic circulation changes at middle latitudes since the Last Glacial Maximum (LGM).

We determined R_{surf} at seven points during the past 16,000 $^{14}C_{atm}$ years (Fig. 2) (10). Five had values similar to the modern one during the Holocene, the Younger Dryas (YD), and the LGM. The Mediterranean R_{surf} value during YD would indicate that the young subtropical Atlantic waters enter into the Mediterranean Sea. However, their reduced advection to the northern North Atlantic north of the polar front (PF) (18) (Fig. 1) and the reduction of atmosphere-ocean CO_2 exchange because of the presence of sea ice could account for the increase of R_{surf} up to ~700 to 800 years (3). Thus, values of R_{surf} during YD on both sides of the PF reflect a strong latitudinal ^{14}C gradient in the North Atlantic, as observed today in the North and South Pacific (2).

Two R_{surf} values at the beginning of the deglaciation were larger than the modern values by a factor of about 2 (Fig. 2) (10). They are estimated as 820 ± 120 years at ~17,000 cal yr B.P. and 810 ± 130 years at ~15,700 cal yr B.P. Such changes were not due to enhanced discharge of ^{14}C-depleted water from the Po river, as shown by the lack of evidence for input of freshwater plants like those that appeared during the following warm climatic interval of the Bölling/Alleröd (B/A) (19) and by SST estimates and analyses of the pollen in this core, which show that the period between 17,000 and 15,000 cal yr B.P. [referred to the Oldest Dryas (OD)] (Fig. 2) (19) was cold and dry.

The two high values of R_{surf} occurred during the massive North Atlantic ice discharge event Heinrich 1 (H1) (20). This event did not modify surface water exchange between the Atlantic and the Mediterranean (13, 21) or the formation of MOW (16, 17). Therefore, these high R_{surf} values cannot be related to a modification of Atlantic-Mediterranean circulation. Furthermore, Adkins *et al.* (7) determined from benthic corals a rapid ^{14}C aging of 670 years of western North Atlantic intermediate water at 15,410 cal yr B.P. (Fig. 1). Taking into account dating uncertainties, we suggest that the two observed increases of the Mediterranean surface and North Atlantic intermediate waters are contemporaneous at around 15,400 to 15,700 cal yr B.P., and are thereby linked.

Possible causes of ^{14}C aging of surface waters are atmospheric ^{14}C fluctuations (related either to production changes such as solar modulation of cosmic rays or to variation of the geomagnetic field) and redistribution within carbon reservoirs (1). No large production changes are observed during the interval 17,000

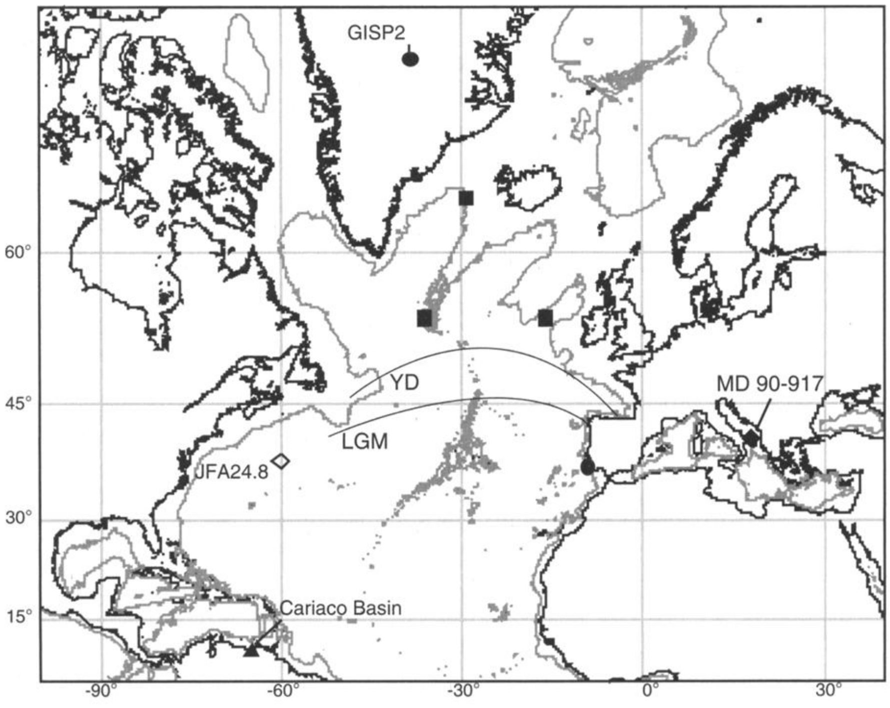

Fig. 1. Locations of core MD 90-917 and of the sites cited in the text: squares from (3), diamond from (7), circle from (26), Cariaco Basin in (29), GISP2 in (30). Position of the polar front is shown for the LGM and the YD (18).

---

[1]Laboratoire des Sciences du Climat et de l'Environnement (LSCE), [2]Unité Mixte de Service, CNRS, Avenue de la Terrasse, F-91118 Gif-sur-Yvette, France. [3]Centro di Studio per la Geologia Strutturale e Dinamica dell' Appennino, [4]Dipartimento di Scienze della Terra, Consiglio Nazionale delle Ricerche (CNR), Via S. Maria 53, 56126 Pisa, Italy. [5]TotalFina Elf, Centre Scientifique Jean Feger, F-64018 Pau, France.

*Present address: Laboratoire de Géochimie des Roches Sédimentaires Université de Paris XI–Orsay, France.

†To whom correspondence should be addressed. E-mail: martine.paterne@lsce.cnrs-gif.fr

to 15,000 cal yr B.P. (*1, 8*). Moreover, modern ocean-atmosphere carbon exchange patterns show that transient reequilibration lasts only a few decades (*2*), so rapid production changes are not expected to account for such a large R_{surf} increase. Greater sea-ice coverage during cold climatic periods would have decreased atmosphere-ocean CO_2 exchange, permitting a local R_{surf} increase of ~200 to 300 years (*22*), but south of the PF (Fig. 1) (*18*) it cannot explain the increase of R_{surf}.

Older surface water reservoir ages may also result from changes in atmospheric CO_2 partial pressure or in wind strength, or from variations of CO_2 exchange between surface water and underlying intermediate water. But none of these fluctuations would have changed reservoir ages by more than 100 years (*2, 3, 23*); only a lowering of the $^{14}C/^{12}C$ in the intermediate water would substantially increase the R_{surf} of the North Atlantic. As derived from the equilibrium equation for a surface water mass (*23*), R_{surf} could then increase up to ~800 years with an age of ~1410 years for intermediate water.

Assuming that both Atlantic intermediate water (*7*) and Mediterranean surface water aged contemporaneously at ~15,700 to 15,400 cal yr B.P., we estimated the intermediate water reservoir age (R_{interm}) or the apparent ventilation age by subtracting the atmospheric ^{14}C age of the Lagno Amendolare tephra [13,070 years (*10*)] from the marine ^{14}C age of the benthic coral [14,520 years; JFA24.8 in (*7*)]. R_{interm} is 1450 ± 100 years, in contrast to the modern value of ~650 years (*24*). The amplitude of this increase (800 ± 100 years) is similar to the increase of 670 ± 60 years measured for North Atlantic intermediate water (*7*), supporting our contention that the R_{surf} change of ~800 years at ~15,400 to 15,700 cal yr B.P. may be explained by the R_{interm} increase.

During H1, the presence of fresh water at high latitudes led to a reduction or a cessation of the Glacial North Atlantic Intermediate Water (GNAIW) formation (*17, 25*). In the North Atlantic at ~2000 m, this event is marked by a rapid and large decrease of benthic $\delta^{13}C$ values (*17, 25*) and high Cd/Ca in benthic corals (*7*), attributed to an input of nutrient-rich and ^{14}C-depleted Antarctic water (*7, 17, 25*). Depleted $\delta^{13}C$ values also have been observed at ~1000 m both off the Portugal margin (*26*) and in the Caribbean (Fig. 1). The presence of old Antarctic water in upper intermediate waters at low to middle latitudes would cause an increase in R_{surf}. The ~1450-year-old R_{interm} would then result either from an older age of the Southern component near the source, which has a modern age of ~800 to 1000 years (*27*), and/or from aging during northward transport from the Southern Ocean to the Northern Atlantic (*7*). This cannot yet be resolved, but aging of the Southern component source is not unrealistic, because the glacial oceanic circulation pattern differed greatly from the modern one (*28*). Moreover, Sikes *et al.* (*5*) measured large ^{14}C changes in the southwest Pacific in the glacial period.

Beyond ~13,000 cal yr B.P., the radiocarbon age calibration (*8*) is mainly based on the U-Th and ^{14}C dates of Atlantic and Pacific low-latitude surface corals and on the Cariaco marine varved sediments (*29*), and does not take into account past R_{surf} changes. However, an increase of R_{surf} would lead to an underestimation of the absolute ^{14}C age difference between 17,000 and 15,000 cal yr B.P. Because the Cariaco record is limited to the past ~15,000 cal yr B.P. (*29*), we checked this possibility by comparing the Greenland Ice Sheet Project GISP2 (*30*) and Adriatic Sea climatic records (Fig. 3). Except for a cold signal at ~6300 cal yr B.P., the first-order and most of the second-order changes, particularly the short cold signal at 8200 cal yr B.P. (*30, 31*), occurred contemporaneously. The good match of the YD age boundaries further argues for the absence of R_{surf} aging of Atlantic surface water at mid-latitudes. A chronology derived from the measured R_{surf} (*10*) also permits us to date the OD-to-B/A transition at 14,560 ± 190 cal yr B.P., in close agreement with the age determined from GISP2 (*30*). Similarly, although dating uncertainties of the GISP2 [±520 years in (*30*)] and Mediterranean [±300 years (*10*)] records are large relative to the observed age

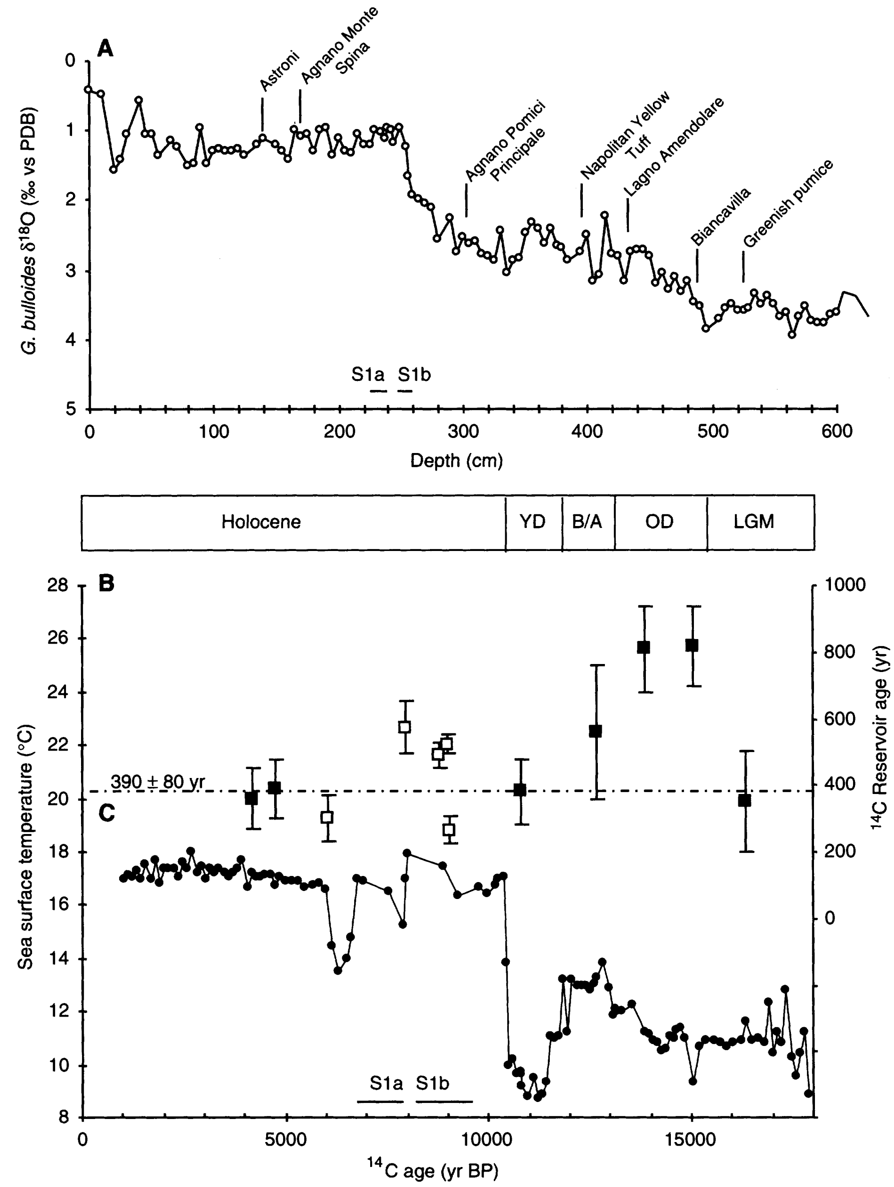

Fig. 2. (**A**) Variations in $\delta^{18}O$ (per mil versus Pee Dee belemnite standard) of *Globigerina bulloides* versus depth. Thick black lines mark the tephra layers (*10*). (**B** and **C**) R_{surf} [(B), right axis] in the South Adriatic Sea (black squares) and from paired marine shells and charcoals in caves (squares) (*4, 9*) and SST [(C), left axis] versus conventional uncorrected ^{14}C ages. The calendar ages are given in Web table 1 (*10*). S1a and S1b refer to the two-step sapropel deposition (9). Climatic transitions are defined by pollen changes (*19*) (YD, Younger Dryas; B/A, Bölling/Alleröd; OD, Oldest Dryas; LGM, Last Glacial Maximum).

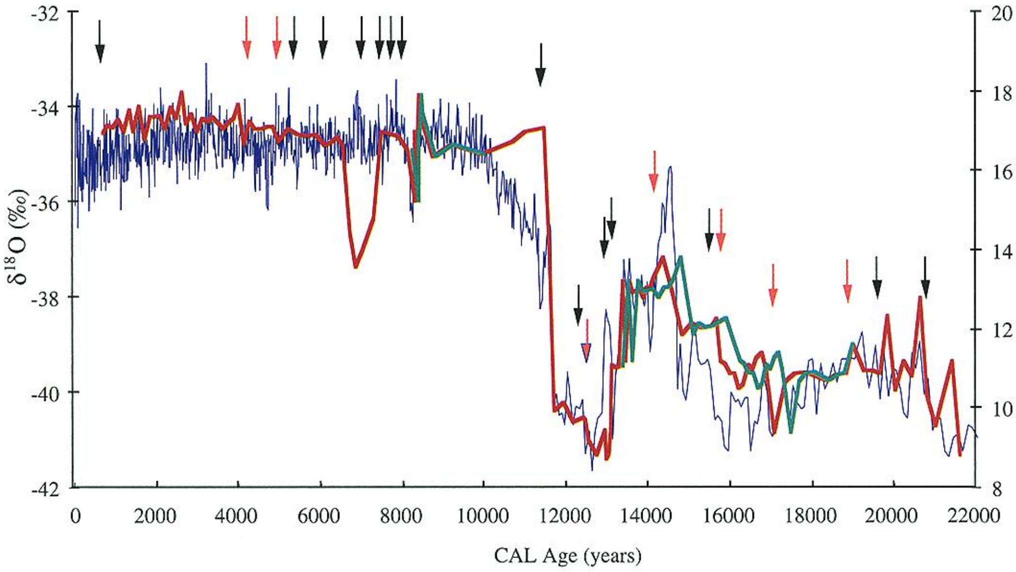

Fig. 3. Comparison of paleoclimatic records from GISP2 (*30*) (blue line) and from MD 90-917 versus cal yr B.P. Chronology of the SST record is obtained by linear fits between two successive AMS ^{14}C ages on tephra (red arrows) and within peaks of abundance of planktonic foraminifera (black arrows) (*9, 11*). The ^{14}C ages were corrected from the varying measured R_{surf} (red line) (*10*) and using a constant R_{surf} of 390 years (*14*) (green line), then converted to calendar ages (*8*). The use of the ~520-year R_{surf} estimate at ~8200 years (*4*), slightly older than the modern one during the sapropel event, permits a better correlation between the two records.

shifts (Fig. 3), a better correlation, particularly in the steepness of the cold-to-warm transition at ~15,600 cal yr B.P., is obtained by using a R_{surf} of ~800 years between 15,000 and 17,000 cal yr B.P. The large R_{surf} values at 17,000 and 15,700 cal yr B.P. could correspond either to a pervasive feature of H1 or to separate short events. Adkins *et al.* (*7*) pointed out that R_{interm} would have changed rapidly in ~160 years from the estimate of the lifetime of modern benthic corals. Hence, the H1 event may have constituted a succession of short surges and therefore a balance of rapid invasion and retreat between the Southern intermediate waters and the GNAIW. Atlantic R_{surf} changes would then be attributable to the rapid resumption and cessation of thermohaline convection (*23*).

References and Notes

1. M. Stuiver, T. F. Braziunas, B. Becker, B. Kromer, *Quat. Res.* **35**, 1 (1991).
2. E. Bard, *Paleoceanography* **3**, 635 (1988).
3. E. Bard *et al.*, *Earth Planet. Sci. Lett.* **126**, 275 (1994).
4. Y. Facorellis, Y. Maniatis, B. Kromer, *Radiocarbon* **40**, 963 (1998).
5. E. L. Sikes, C. R. Samson, T. P. Guilderson, W. R. Howard, *Nature* **405**, 555 (2000).
6. W. S. Broecker *et al.*, *Paleoceanography* **3**, 659 (1988).
7. J. F. Adkins, H. Cheng, E. A. Boyle, E. R. Druffel, R. L. Edwards, *Science* **280**, 725 (1998).
8. M. Stuiver *et al.*, *Radiocarbon* **40**, 1041 (1998).
9. G. Siani, thesis, Université de Paris-Sud Orsay (1999).
10. See supplementary Web material at *Science* Online (www.sciencemag.org/cgi/content/full/294/5548/1917/DC1).
11. D. Mercone *et al.*, *Paleoceanography* **15**, 336 (2000).
12. The peaks of abundance of glass shards and of foraminifera do not show the distribution tails (*9*), as is characteristic of bioturbation processes. Using sample resolution, sedimentation rate, and the assumption of a content of 100% glass shards before bioturbation (*32*), the aging ranges from 30 years (with a mixing depth of 2 cm) to 80 years (with 4 cm); these values are negligible with respect to R_{surf} age changes and associated uncertainties (*10*).
13. N. Kallel, M. Paterne, L. D. Labeyrie, J. C. Duplessy, M. Arnold, *Palaeogeogr. Palaeoclimatol. Palaeoecol.* **135**, 97 (1997).
14. G. Siani *et al.*, *Radiocarbon* **42**, 271 (2000).
15. W. S. Broecker, R. Gerard, *Limnol. Oceanogr.* **14**, 883 (1969).
16. R. Zahn, M. Sarnthein, H. Erlenkeuser, *Paleoceanography* **2**, 543 (1987).
17. M. Sarnthein *et al.*, *Paleoceanography* **9**, 209 (1994).
18. W. F. Ruddiman, A. McIntyre, *Palaeogeogr. Palaeoclimatol. Palaeoecol.* **35**, 145 (1981).
19. N. Combourieu-Nebout, M. Paterne, J. L. Turon, G. Siani, *Quat. Sci. Rev.* **17**, 303 (1998).
20. G. Bond *et al.*, *Nature* **360**, 245 (1992).
21. I. Cacho *et al.*, *Paleoceanography* **14**, 698 (1999).
22. T. F. Stocker, D. G. Wright, *Radiocarbon* **40**, 359 (1998).
23. To test the sensitivity of the R_{surf} age to carbon exchange with the atmosphere and the underlying intermediate water, we wrote a simplified equilibrium equation of a surface water ^{14}C/^{12}C ratio. The equation and results are discussed in (*10*).
24. W. S. Broecker, T. H. Peng, S. Trumbore, G. Bonani, W. Wolfli, *Global Biogeochem. Cycles* **4**, 103 (1990).
25. L. Vidal *et al.*, *Clim. Dyn.* **15**, 909 (1999).
26. R. Zahn *et al.*, *Paleoceanography* **12**, 696 (1997).
27. H. G. Ostlund, C. Craig, W. S. Broecker, D. Spencer, Eds., *GEOSECS Atlantic, Pacific, and Indian Ocean Expeditions. Shorebased Data and Graphics, GEOSECS Expedition, 7* (U.S. Government Printing Office, Washington, DC, 1987).
28. E. Michel *et al.*, *Paleoceanography* **10**, 927 (1995).
29. K. A. Hughen *et al.*, *Radiocarbon* **40**, 483 (1998).
30. R. B. Alley *et al.*, *Nature* **362**, 527 (1993).
31. U. von Grafenstein *et al.*, *Science* **284**, 1654 (1999).
32. E. Bard *et al.*, *Clim. Dyn.* **1**, 101 (1987).
33. We acknowledge helpful comments from T. Goslar, J. Cochran, D. Paillard, M. Fontugne, P. Jean-Baptiste, and Institut Français de Recherche et Technologie Polaire for Marion Dufresne coring facilities. Supported by Ministero Italiano degli Affari Esteri (G.S.), CNR (R.S.), CNRS and Commissariat à l'Energie Atomique, and the Marine and Science Technology IIIrd program–Clivamp and the Institut National des Sciences de l'Univers: Environment et Climat du Passé: Histoire et Evolution programs of the European Union. This is LSCE Contribution number 685.

20 June 2001; accepted 10 October 2001

Effects of Marine Reserves on Adjacent Fisheries

Callum M. Roberts,[1,2]* James A. Bohnsack,[3] Fiona Gell,[2]
Julie P. Hawkins,[2] Renata Goodridge[4]

Marine reserves have been widely promoted as conservation and fishery management tools. There are robust demonstrations of conservation benefits, but fishery benefits remain controversial. We show that marine reserves in Florida (United States) and St. Lucia have enhanced adjacent fisheries. Within 5 years of creation, a network of five small reserves in St. Lucia increased adjacent catches of artisanal fishers by between 46 and 90%, depending on the type of gear the fishers used. In Florida, reserve zones in the Merritt Island National Wildlife Refuge have supplied increasing numbers of world record–sized fish to adjacent recreational fisheries since the 1970s. Our study confirms theoretical predictions that marine reserves can play a key role in supporting fisheries.

Marine reserves, areas that are closed to all fishing, have been attracting much attention for their dual potential as conservation and fishery management tools (*1–5*). A synthesis of more than 100 studies of reserves worldwide shows that protection from fishing leads to rapid increases in biomass, abundance, and average size of exploited organisms and to increased species diversity (*6*). Such effects are of great interest to fishery managers, because rebuilding